energies

MDPI

Article

Mooring Angle Study of a Horizontal Rotor Wave Energy Converter

Zhongliang Meng [1], Yanjun Liu [1,*], Jian Qin [1] and Shumin Sun [2]

[1] Key Laboratory of High Efficiency and Clean Mechanical Manufacture, Ministry of Education, Institute of Marine Science and Technology, School of Mechanical Engineering, Shandong University, Qingdao 266237, China; 201720545@mail.sdu.edu.cn (Z.M.); qinjian1997@163.com (J.Q.)

[2] State Grid Shandong Electric Power Company Electric Power Science Research Institute, Jinan 250002, China; meng198512@126.com

* Correspondence: lyj111@sdu.edu.cn; Tel.: +86-133-2513-6508

Abstract: The horizontal rotor wave energy converter is a newly designed wave energy converter. While the mooring system plays a vital role in keeping the device floating stably, the selection of the mooring angle has immediate effects on the device's floating stability and energy generation efficiency. Given the properties of wave energy along the coast in Shandong Province, this study combines wave statistics gathered from field measurements of a certain area in the Bohai Sea with hydrological data obtained in a field test in the same sea area and adopts Stokes' fifth-order wave theory to theoretically design and simulate the mooring system for the new type of power generating device. With the help of AQWA software, data on the dynamics of the device at various angles are obtained to construct models and carry out regular wave experiments according to the most appropriate mooring angles to show the validity of the selected mooring angles. The consistency of the results between the experiment and simulation confirms that under the same working conditions of regular waves, as the mooring angle increases, the roll angle decreases first and then increases, the pitch angle barely varies, and the yaw angle decreases first and then increases. The adoption of this simulation method and the gathered experimental data help to provide theoretical and practical bases for choosing the mooring method for the engineering prototype and obtaining a reliable supply of power.

Keywords: wave energy; horizontal rotor; mooring angle; regular wave; hydrodynamic response

Citation: Meng, Z.; Liu, Y.; Qin, J.; Sun, S. Mooring Angle Study of a Horizontal Rotor Wave Energy Converter. *Energies* **2021**, *14*, 344. https://doi.org/10.3390/en14020344

Received: 13 December 2020
Accepted: 7 January 2021
Published: 9 January 2021

1. Introduction

Since the start of the 21st century, international energy consumption has seen a sustained increase and a strained relationship between supply and demand. International disputes brought on by the scarcity of resources and energy have become not only one of the hot topics of national and global competition but also a critical element that constrains the economic growth of countries and the world as a whole [1,2]. Since the beginning of the industrial revolution, the use of traditional fossil fuel has caused haze, fog, dust, and greenhouse effects among other environmental issues. The emission of carbon dioxide has increased the global temperature by 1 °C and the trend will continue until at least the end of the century. Therefore, the utilization of new energy sources has gradually been placed on the agenda of every country. The Global Energy Statistics Report published by BP in 2019 pointed out that global carbon emissions reached a peak in 2018 relative to the prior seven years. As the demand for primary energy sources has climbed dramatically, the growth of the need for energy in 2018 became the fastest it had been over the preceding decade, with energy consumption increasing by 2.9%. In the report, it is estimated that because of the steady economic growth of developing countries and the enhanced awareness of environmental protection, as well as increasingly diversified energy, the average growth of global energy demand will be 1.3% by 2040, lower than that in the past two decades [3–5].

The use of renewable energy can change the way traditional energy is consumed and thus benefits environmental protection [6]. As the largest developing country and the second-largest economy in the world, China has witnessed rapid economic growth and increasingly rising energy consumption at the same time. Nevertheless, energy acts as a guarantee for economic development in China and a necessity for daily life [7,8]. The report published by the 18th CPC National Congress put forward for the first time a strategic goal of establishing China as a maritime power. The 19th CPC National Congress further implemented a policy of stepping up the increase in maritime power. Additionally, the 13th Five-Year Plan for Marine Renewable Energy Development published by China in 2017 stated that by 2020, the key technological equipment for marine energy will realize stable generation and the installed capacity will reach 5×10^4 kW; the plan also stated five basic missions related to the integration of marine development and the Belt and Road Initiative [9,10].

The common structural forms of wave-energy-generating devices include the oscillating water column, overtopping device, and oscillating body [11–15]. The new horizontal rotor wave-energy-generating device adopts the generation principle of a crossflow turbine, as shown in Figure 1. The device's installed capacity is 6 kW, its rated generating capacity is 1.1 kW, and it weighs approximately 28 tons [16]. The device forms a closed body of water through the entry and exit passages of the crossflow turbine. As a result of the strike and backflow of the wave, the water body in the passage flows back and forth, which drives the rotor in the passage to rotate in one direction and makes the direct-drive generator produce electricity. An engineering prototype is shown in Figure 2. Many countries have made plans to develop wave energy and have also developed various wave energy converters. Researchers in the US, Europe, and Australia previously developed these technologies, therefore, some have already been commercially operated [17–20]. The Korea Maritime and Ocean University developed a floating horizontal-axis wave energy model device that utilizes mainly the rise and fall of water on the flanks of the turbine that follows the movement of the waves to rotate the turbine and then uses the driving force to power devices through a force transmitter. The device has not yet been made into an engineering prototype [21]. Wuhan University and the Chinese Academy of Sciences jointly developed a 1 kW vertical-axis tidal-current-energy-generating device and conducted marine experiments in the sea area of Zhuhai. Shanghai Ocean University designed a horizontal-axis-generating device and conducted a series of experiments in the sea areas of Xiamen [22]. Harbin Engineering University developed a vertical-axis tidal-current-energy-generating device [23,24]. Furthermore, Zhejiang University and Ocean University of China both carried out engineering prototype experiments and achieved some results [25]. As the application of wave-energy-generating devices is in the preliminary stage, studies of their mooring systems both at home and abroad are thus very rare. Therefore, simulations and experiments are typically performed on a semisubmersible platform, floating wind generator, or other floating marine structures. Wang Kun [26] and Chen Fei [27] studied the states of motion of a three- and single-point mooring system. Hou Huimin [28] conducted a reliability assessment of seawater culture cages under extreme conditions. Carlos Barrera [29], Pham [30], and Shen [31] carried out studies on the dynamics of the mooring system of a floating wind turbine. Ghafari [32] and Xutian Xue [33] studied the mooring method of a semisubmersible platform. Existing data indicate that many studies have been performed on the deep sea and on deep-sea mooring devices, while little research has been conducted on shallow-water mooring for near-shore power generation devices. In this paper, based on the sea conditions under which the device will be operated, a preliminary discussion on the shallow-water mooring angle of the new power generation device is conducted, and experiments on the mooring stability of the new power generation device are analyzed.

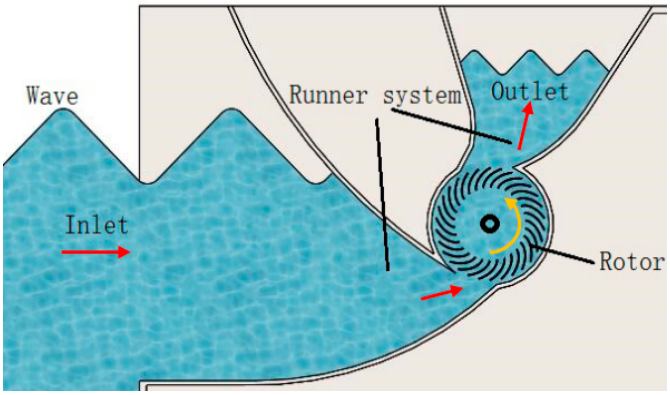

Figure 1. Cutaway view of the device.

Figure 2. Engineering prototype.

As the device must be moored to operate in a severe marine environment for a long period, it should be able to resist extreme storms and be economical in design to ensure that the device is secure and stable as well as efficient in capturing wave energy [34,35]. The studies on this new device in China were all relatively recent and lacked special standards, so the device design mainly refers to floating marine structures such as semisubmersible platforms, culture cages, floating wind turbines, and tension leg platforms [36–41]. To restrict the drift of the wave energy device during its operation in an extreme state, compared with other large floating structures, the device has some requirements in the design of its mooring system. For example, the device should be set as far as possible against the current to capture wave energy in a highly efficient manner; the device should be able to keep its relative stability given the combined dynamic motions of the wind, wave, and current; and damage to the mooring system caused by enormous stress should be avoided as much as possible [42–44].

2. Principal Basis

The experiment on the engineering prototype was carried out in a certain area of the Bohai Sea, as shown in Figure 3 [8]. Its longitude is N37026′29″ and its latitude is E122035′4″. According to wave data of the sea areas neighboring Weihai in 2016, 2017, and 2018 from the Monthly Report of China's Offshore Marine Climate Monitoring provided by the National Marine Environmental Forecasting Center, the significant wave height of the sea area during the three years was 0.75 m, and the significant wave period was 3.9 s [45].

The water depth at the location where the generating device was tested was 15 m [46] After calculation, Stokes' second-order wave theory was applied theoretically to the tested sea area [47,48].

Figure 3. Chengshantou sea trial area.

Mooring methods are classified into catenary mooring and tensioned mooring. Catenary mooring can restrict the motion of the platform with the gravity of catenaries, so this method is usually adopted by marine-energy-generating devices. Based on the new device's bilateral symmetry, three layout schemes are selected for the mooring system: the anchor chains are bilaterally symmetric and the angles between the first anchor chain and the wave are 30°, 45°, and 60°. The layout is shown in Figure 4.

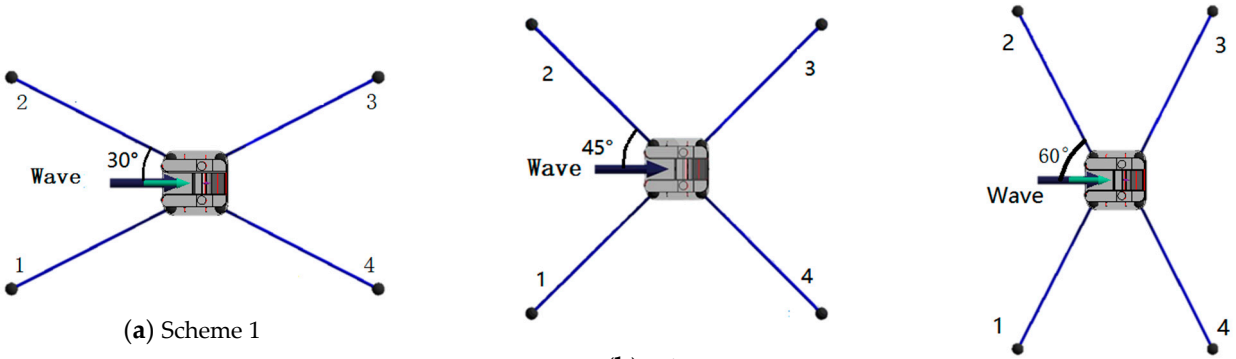

(**a**) Scheme 1 (**b**) Scheme 2 (**c**) Scheme 3

Figure 4. Mooring schemes.

To ensure the stability of the device, a four-point mooring method is adopted. The device floats on the sea surface, and the damping plate under the device connects to the sea bottom through anchor chains to ensure the stability and balance of the device when wind and waves strike it. The water depth in the area where the device was tested is 15 m, and the device displaces water to a depth of 4.7 m; therefore, the vertical length of the anchor chains is 10.3 m. The weight of the chains is 7/8 of their weight in a vertical position. There are four anchor chains with a total vertical length of 41.2 m. According to the prototype of the anchor chains, each chain's diameter is 50 mm and weight is 49.5 kg/m, so the total weight is 2040 kg, and the weight of the chains in the water is approximately 1759 kg when the buoyant force is excluded [49].

Dangling chain length:

$$S_h = \sqrt{\frac{2HT_0}{q_w} + H^2}. \quad (1)$$

In the above formula, H refers to the vertical distance from the ground of the anchor point to the anchor hole; T_0 is the tension at the ground end of the hanging chain; and q_w is the wet weight of the anchor chain per unit length in water.

$$T_0 = P_a + P_w. \tag{2}$$

In the above formula, P_a is the acting force of wind applied to the device and P_w is the acting force of the water flow applied to the device.

$$P_a = \frac{1}{2}\rho_a C_a V_a^2 \left(A_a cos^2\theta + B_a sin^2\theta \right). \tag{3}$$

In the above formula, ρ_a is the density of the air, 1.25 kg/m^3; C_a is the wind factor, 0.70–0.95; V_a is the relative wind speed; A_a is the area of the device above the waterline; B_a is the flanking area of the device above the waterline; and θ is the angle of the chord between the device and the wind.

$$P_w = f \cdot \Omega \cdot V_w^{1.88}. \tag{4}$$

In Froude's formula above, f is the water's friction coefficient, $f = 0.17$; V_w is the speed of water flow; and Ω is the wet surface area of the device below the waterline.

The length of anchor chains in the water:

$$S_b = {}^1/_2 S_h. \tag{5}$$

The total length of anchor chains [50]:

$$S = S_h + S_b = 1.5 S_h. \tag{6}$$

3. Analogue Simulation

In AQWA simulations for hydrodynamic research, the research object is a rotor wave energy capture device with upper and lower structures. Physical modeling is carried out through ANSYS/APDL. The main body is divided into the main floating body and the damping plate. The main dimensional parameters are shown in Table 1. The model grid division is shown in Figure 5. The model is divided into 21,750 grids, and the wave type is set to a Stokes second-order wave. AQWA software was used to carry out a coupling simulation analysis of the device when the wind, wave, and flows are in the same direction while inputting the following data: the total length of the single anchor chain is 23.13 m, the significant wave period is 3.6 s, the significant wave height is 0.70 m, the wind speed is 6 m/s, and the speed of water flow is 2/s. An irregular wave simulation can be set to the Pierson–Moskowitz spectrum.

Table 1. The main size parameters of the rotor wave energy capture device.

Device Parameters	Prototype Data	Unit
Total height of the device	5.443	m
Length of the main float	6.000	m
Width of the main float	4.412	m
Height of the main float	2.948	m
Damping disc length	6.000	m
Damping disc width	6.000	m
Damping plate height	2.495	m
Depth of the draft	4.697	m
Center of gravity height	2.684	m
Displacement	30,900.000	kg

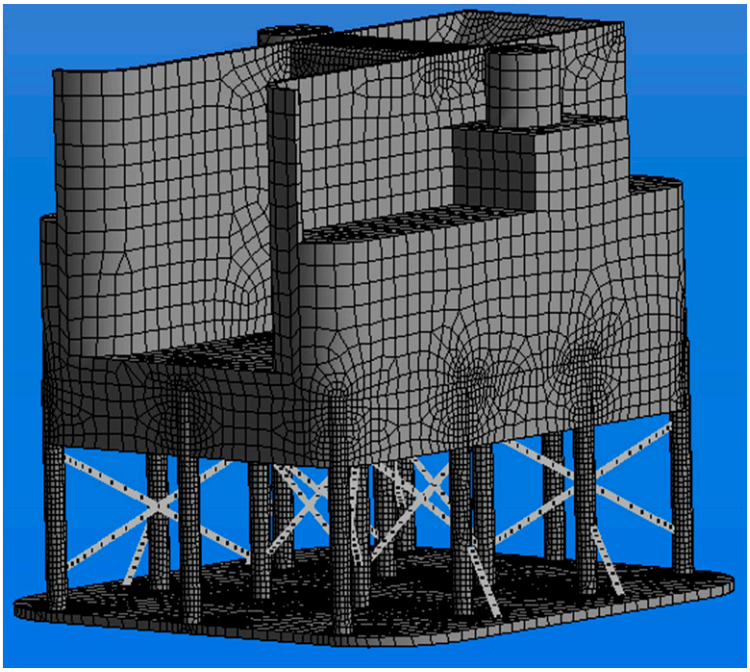

Figure 5. Meshing.

According to the sea conditions in the test area, the working condition of the regular wave was set to perform the simulation. The significant wave height is 0.7 m and the significant wave period is 3.6 s, which approximate the actual state of the sea during a certain period. The device's motion in the state of stable floating can be obtained through simulation to analyze the rationality of the mooring angles.

The layout of anchor chains 1 and 2 is symmetric, so the stress changes of the two chains are similar, as shown in Figures 6 and 7. Floating of the device becomes stable after 30 s. The stress of the two chains in scheme 1 barely varies, whereas their stress in scheme 3 varies greatly, and their stress in scheme 2 varies moderately.

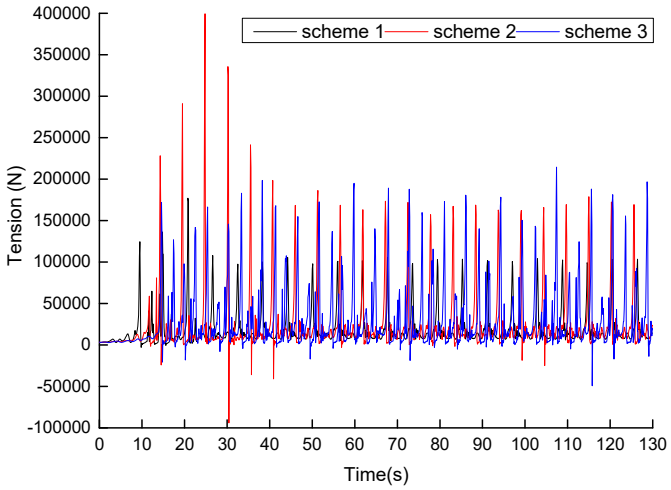

Figure 6. The stress of anchor chain 1 in schemes 1, 2, and 3.

Anchor chains 3 and 4 are also symmetrically laid out, so the stress changes of the two chains are also similar, as shown in Figures 8 and 9. Floating of the device becomes stable after 30 s. The stress of the two chains in scheme 1 varies greatly, whereas their stress in scheme 3 varies moderately, and their stress in scheme 2 barely varies.

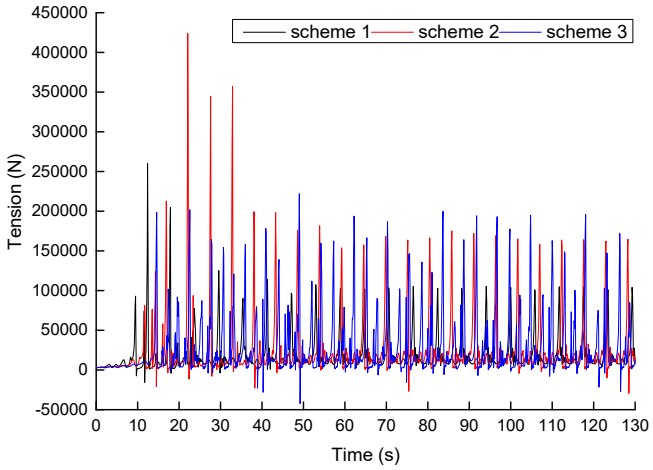

Figure 7. The stress of anchor chain 2 in schemes 1, 2, and 3.

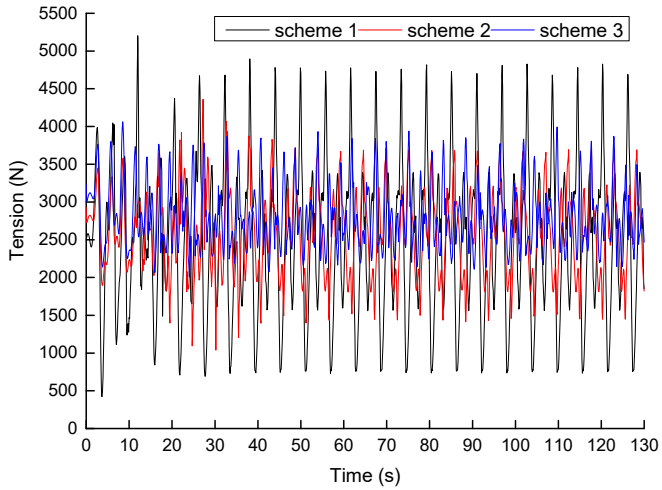

Figure 8. The stress of anchor chain 3 in schemes 1, 2, and 3.

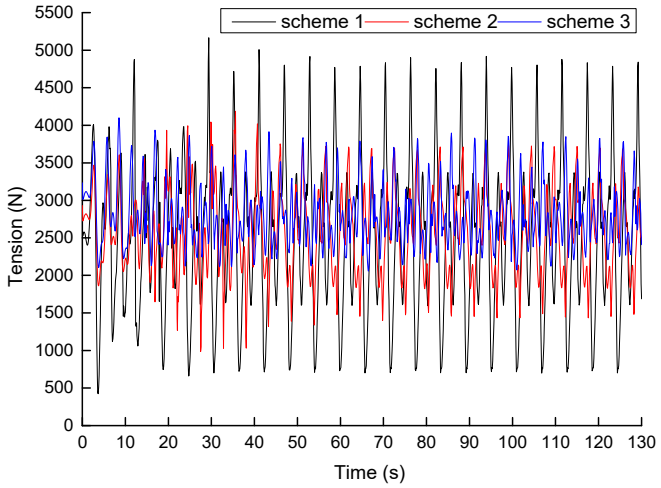

Figure 9. The stress of anchor chain 4 in schemes 1, 2, and 3.

The data obtained by simulating regular wave working conditions demonstrate that the symmetric anchor chains have similar stresses and that mooring scheme 2 is the optimal choice considering the stresses of the anchor chains.

The angle variations of the pitch, roll, and yaw in scheme 1 are shown in Figure 10. The pitch varies by approximately ±9°, the roll varies by ±13°, and the yaw varies by ±20°. The angles of scheme 1 in the RX, RY, and RZ directions vary greatly, which is harmful to the stable generation of the device.

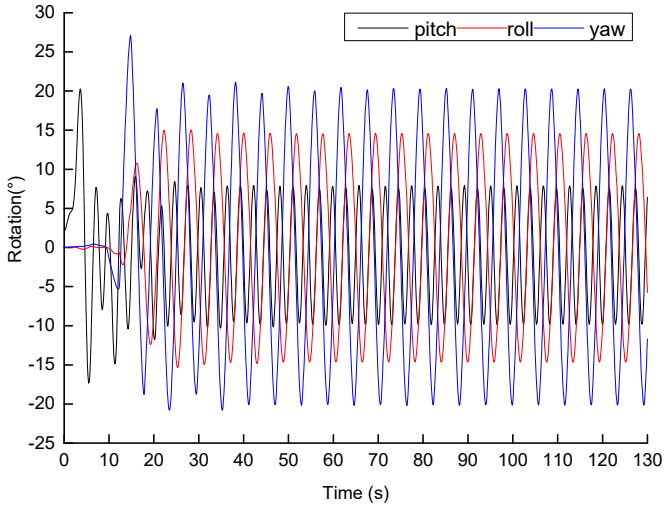

Figure 10. The angle variations of the pitch, roll, and yaw in scheme 1.

The angle variations of the pitch, roll, and yaw in scheme 2 are shown in Figure 11. The pitch varies by approximately ±4°, the roll varies by ±13°, and the yaw varies by ±5°. The pitch angles vary slightly, which will help the device embrace head-on waves and absorb their energy. The angles of scheme 2 in the RX, RY, and RZ directions benefit the stable floating of the device, making scheme 2 the optimal choice.

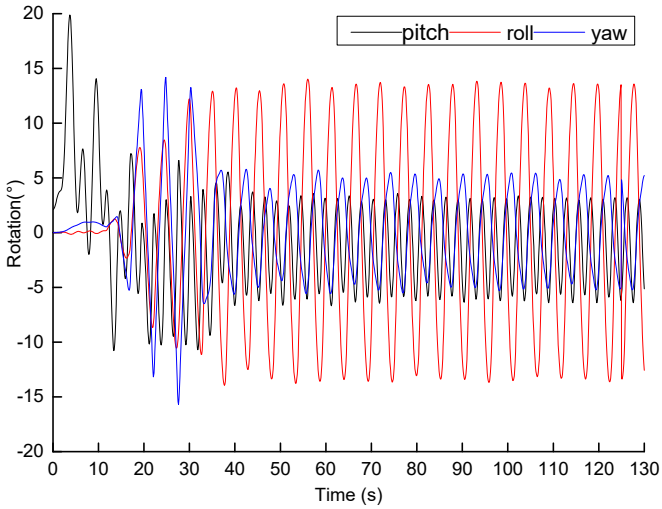

Figure 11. The angle variations of the pitch, roll, and yaw in scheme 2.

The angle variations of the pitch, roll, and yaw in scheme 3 are shown in Figure 12. The pitch varies by approximately ±8°, the roll varies by ±9°, and the yaw varies by ±9°. Although the roll and yaw angles do not vary greatly, its angle variation of the pitch is not as appropriate as in scheme 2. Therefore, scheme 2 is selected as the most practical mooring scheme from the sea experiment.

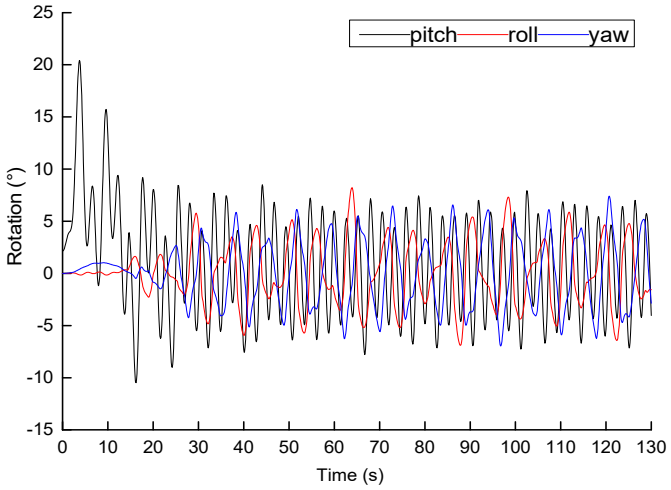

Figure 12. The angle variations of the pitch, roll, and yaw in scheme 3.

4. Experiment Validation

A test of the model was carried out in the wave-current coupling water trough at the National Engineering Laboratory. Considering the principle of similarity, the background of the engineering construction, and the conditions of the water trough, the tested model has a scale of 1:10 and the design of the anchor chains should resemble those of the prototype in length, mass, and elasticity. The experimental conditions of the wave generation water tank are set based on the principle above (Table 2).

Table 2. Experiment condition.

Experiment Condition	Prototype Value		Model Value	
Parameter	Wave Height H (m)	Cycle T (sec)	Wave Height H (m)	Cycle T (sec)
Case	0.7	3.6	0.07	1.15

The experiment conducted on the model is depicted in Figure 13a,b. According to the actual state of the sea, the device's motion becomes stable after 10 s, so the time interval selected to validate the accuracy of the simulated data is 25 s. The whole device is hoisted and placed in the experimental tank. The data acquisition device uses a fifth-generation attitude motion tester developed by the Norwegian Kongsberg Maritime Company; it is an inertial attitude reference system with dynamic linear motion that can dynamically test the six models of the prototype. The parameters, such as the degrees of freedom and the angular velocity vector, are shown in Figure 13c. The data sampling period is 0.04 s. After the device is adjusted to the initial state, it starts to continuously sample the motion data.

Figure 14 shows the angle variations of scheme 1 in the mooring experiment. In the regular wave experiment, the device swings under the impact of regular waves. The maximum pitch angle is approximately equal to 8.9°, and the average value is about 8.08°. The maximum roll angle is approximately equal to 12.2°, and the average value is about 11.28°. The maximum yaw angle is approximately equal to 20.3°, and the average value is about 19.99°.

Figure 15 shows the angle variations of scheme 1 in the mooring experiment. The maximum pitch angle is approximately equal to 5.7°, and the average value is about 5.08°. The maximum roll angle is approximately equal to 12.2°, and the average value is about 11.28°. The maximum yaw angle is approximately equal to 5.3°, and the average value is about 4.99°.

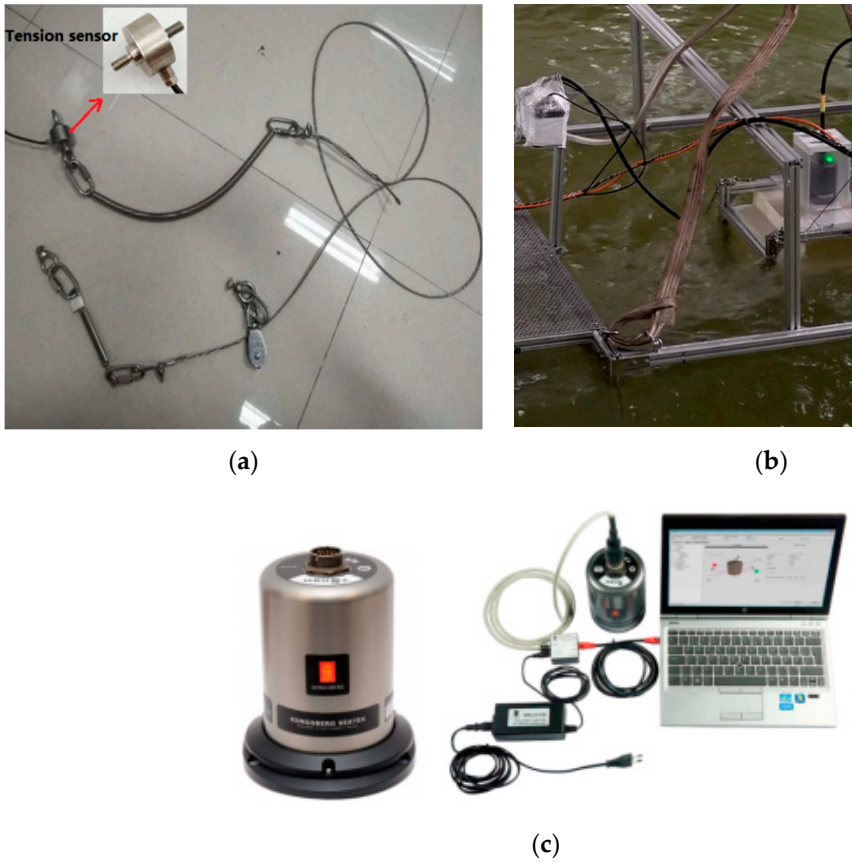

Figure 13. Mooring experiment: (**a**) anchor chains; (**b**) model test; (**c**) 5th generation motion reference unit.

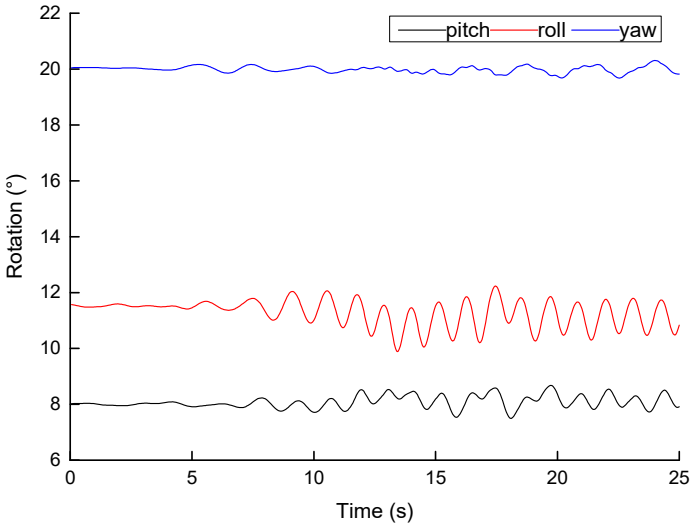

Figure 14. The angle variations of scheme 1 in the mooring experiment.

Figure 16 shows the angle variations of scheme 1 in the mooring experiment. The maximum pitch angle is approximately equal to 8.7°, and the average value is about 8.08°. The maximum roll angle is approximately equal to 9.3°, and the average value is about 8.28°. The maximum yaw angle is approximately equal to 7.3°, and the average value is about 6.99°.

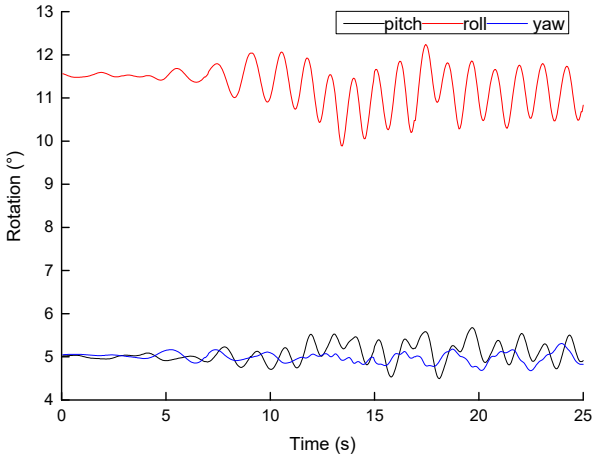

Figure 15. The angle variations of scheme 2 in the mooring experiment.

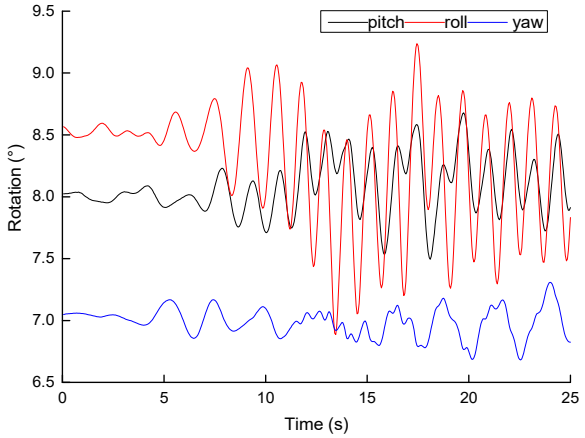

Figure 16. The angle variations of scheme 3 in the mooring experiment.

The average value of rotation angles is shown in Table 3. Figure 17 shows the stability influence of mooring angle for the device. As the mooring angle increases, the pitch angle decreases first and then increases, the roll angle barely varies, and the yaw angle decreases first and then increases. The combined model has the smallest change in pitch amplitude because the combined model is fluid adaptive and has the smallest rotation range due to the mooring effect of the anchor chain. It can be seen that the average value of rotation angles in scheme 2 is smaller, indicating that scheme 2 is more reasonable. In order to obtain more accurate data in the experiment, the tension sensor with higher accuracy can be applied to replace the original one, or the model's center of gravity can be adjusted several times. In the future, the experimental method will be optimized continually.

Table 3. Mean value of device rotation.

Rotation Angle	Average Value (°)		
	Scheme 1	Scheme 2	Scheme 3
Pitch	8.08	5.08	8.08
Roll	11.28	11.28	8.28
Yaw	19.99	4.99	6.99

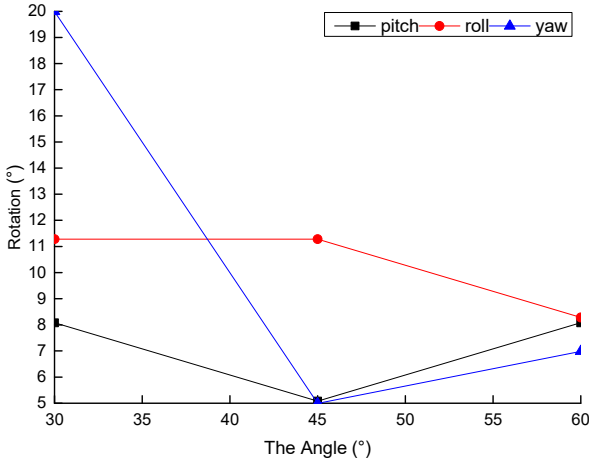

Figure 17. Stability influence of mooring angle for the device.

5. Conclusions

Initially, the mooring angles were carefully selected according to the symmetric structure of the device. After simulating the wind, wave, and current coupling of the generating device, this study confirmed the angle variations of the device under regular wave working conditions and conducted a series of experiments in a water trough. There was no significant change in the pitch amplitude of the combined model because the combined model is fluid adaptive. The pitch motion of the model was determined by the combined model hydrodynamic performance, rotor rotating hydrodynamic characteristics, and mooring cables. The value responses are more complicated. The conclusions are as follows. Under the same working conditions, a comparison of the results between the simulation and experiment demonstrates that the angle's variation scope in the experiment is smaller than that in the simulation because of the lack of wind and the current equipment. Therefore, errors have occurred in the experiment. The simulation results indicate that among the three schemes, the stress variations of the anchor chains in scheme 2 are the most plausible. The consistency of the results between the experiment and simulation confirms that under the same working conditions of regular waves, as the mooring angle increases, the pitch angle decreases first and then increases, the roll angle barely varies, and the yaw angle decreases first and then increases. In view of the experimental data, the mooring angle of scheme 2, that is, 45 degrees, is the most suitable one.

Author Contributions: Conceptualization, Z.M. and Y.L.; methodology, Z.M. and Y.L.; software, J.Q.; validation, Y.L.; investigation, Z.M. and Y.L.; resources, Y.L.; data curation, Y.L.; writing—review and editing, Z.M.; supervision, S.S. All authors have read and agreed to the published version of the manuscript.

Funding: This research was funded by the Science and Technology Project of the State Grid Corporation of China. The grant number of "Research and Demonstration of Key Technologies for Distributed Ocean Renewable Energy Power Generation and Grid Control" is 5400-201916148A-0-0-00.

Acknowledgments: The authors are grateful for the State Grid Corporation of China. In addition, thank you very much for the support provided by the cooperation project of China Institute of Water Resources and Hydropower Research.

Conflicts of Interest: The authors declare no conflict of interest.

References

1. Østergaard, P.A.; Duic, N.; Noorollahi, Y.; Mikulčić, H.; Kalogirou, S. Sustainable Development Using Renewable Energy Technology. *Renew. Energy* **2020**, *146*, 2430–2437. [CrossRef]
2. Segura, E.; Morales, R.; Somolinos, J. A strategic Analysis of Tidal Current Energy Conversion Systems in the European Union. *Appl. Energy* **2018**, *212*, 527–551. [CrossRef]
3. Melikoglu, M. Current Status and Future of Ocean Energy Sources: A global Review. *Ocean Eng.* **2018**, *148*, 563–573. [CrossRef]

4. Roy, A.; Auger, F.; Dupriez-Robin, F.; Bourguet, S.; Tran, Q.-T. Electrical Power Supply of Remote Maritime Areas: A Review of Hybrid Systems Based on Marine Renewable Energies. *Energies* **2018**, *11*, 1904. [CrossRef]
5. Aderinto, T.; Li, H. Ocean Wave Energy Converters: Status and Challenges. *Energies* **2018**, *11*, 1250. [CrossRef]
6. Mwasilu, F.; Jung, J. Potential for Power Generation from Ocean Wave Renewable Energy Source: A Comprehensive Review on State-of-the-Art Technology and Future Prospects. *IET Renew. Power Gener.* **2019**, *13*, 363–375. [CrossRef]
7. Qiu, S.; Liu, K.; Wang, D.; Ye, J.; Liang, F. A Comprehensive Review of Ocean Wave Energy Research and Development in China. *Renew. Sustain. Energy Rev.* **2019**, *113*, 113–109271. [CrossRef]
8. Hou, J.; Zhu, X.; Liu, P. Current Situation and Future Projection of Marine Renewable Energy in China. *Int. J. Energy Res.* **2019**, *43*, 662–680. [CrossRef]
9. Chang, Y.-C.; Wang, N. Legal System for the Development of Marine Renewable Energy in China. *Renew. Sustain. Energy Rev.* **2017**, *75*, 192–196. [CrossRef]
10. National Energy Administration. The 13th Five-Year Plan for Renewable Energy Development (Part 1). *Sol Energy.* **2017**, *2*, 5–11.
11. Liu, Z.; Hyun, B.-S.; Hong, K. Numerical Study of air Chamber for Oscillating Water Column Wave Energy Convertor. *China Ocean Eng.* **2011**, *25*, 169–178. [CrossRef]
12. Doyle, S.; Aggidis, G.A. Development of Multi-Oscillating Water Columns as Wave Energy Converters. *Renew. Sustain. Energy Rev.* **2019**, *107*, 75–86. [CrossRef]
13. Martin, D.; Li, X.; Chen, C.-A.; Thiagarajan, K.; Ngo, K.; Parker, R.G.; Liu, M. Numerical Analysis and Wave Tank Validation on the Optimal Design of a Two-Body Wave Energy Converter. *Renew. Energy* **2020**, *145*, 632–641. [CrossRef]
14. Martins, J.; Goulart, M.; Gomes, M.D.N.; Souza, J.A.; Rocha, L.; Isoldi, L.A.; Dos Santos, E.D. Geometric Evaluation of the Main Operational Principle of an Overtopping Wave Energy Converter by Means of Constructal Design. *Renew. Energy* **2018**, *118*, 727–741. [CrossRef]
15. Phan, C.B. A Study on Design and Simulation of the Point Absorber Wave Energy Converter Using Mechanical PTO. In Proceedings of the 4th International Conference on Green Technology and Sustainable Development (GTSD), Ho Chi Minh City, Vietnam, 23–24 November 2018; pp. 122–125.
16. Guo, X.; Wu, Y. Research on Power Bandwidth Design Method of Direct Drive Turbine Wave Energy Utilization Device. *J. Hydro Eng.* **2013**, *32*, 197–203.
17. Nguyen, H.; Wang, C.; Tay, Z.; Luong, V. Wave Energy Converter and Large Floating Platform Integration: A review. *Ocean Eng.* **2020**, *213*, 107768. [CrossRef]
18. Li, N.; Cheung, K.F.; Cross, P. Numerical Wave Modeling for Operational and Survival Analyses of Wave Energy Converters at the US Navy Wave Energy Test Site in Hawaii. *Renew. Energy* **2020**, *161*, 240–256. [CrossRef]
19. Vieira, F.; Cavalcante, G.; Campos, E.; Taveira-Pinto, F. Wave Energy Flux Variability and Trend Along the United Arab Emirates Coastline Based on a 40-Year Hindcast. *Renew. Energy* **2020**, *160*, 1194–1205. [CrossRef]
20. Mctiernan, K.L.; Sharman, K.T. Review of Hybrid Offshore Wind and Wave Energy Systems. *J Phys Confser.* **2020**, *1452*, 12016. [CrossRef]
21. Kim, B.-H.; Wata, J.; Zullah, M.A.; Ahmed, M.R.; Lee, Y.-H. Numerical and Experimental Studies on the PTO System of a Novel Floating Wave Energy Converter. *Renew. Energy* **2015**, *79*, 111–121. [CrossRef]
22. Ren, W. Dynamic Analysis of Flexible Direct-Drive Wave Power Turbines. Master's Thesis, Shanghai Ocean University, Shanghai, China, 2016.
23. Li, Z. Research on Braking Strategy and Realization Method of Tidal Current Energy Turbine. Master's Thesis, Harbin Engineering University, Harbin, China, 2016.
24. Jing, F. A New Type of Floating Tidal Current Energy Device Hydrodynamic Research. Ph.D. Thesis, Harbin Engineering University, Harbin, China, 2013.
25. Wang, S.; Li, M.; Li, Z. Overview of International Tidal Current Energy Utilization Technology Development. *Ship Eng.* **2020**, *42*, 23–28.
26. Wang, K.; Er, G.-K.; Iu, V.P. Nonlinear Random Vibrations of 3D Cable-Moored Floating Structures Under Seismic and Wave Excitations. *J. Sound Vib.* **2019**, *452*, 58–81. [CrossRef]
27. Chen, F.; Duan, D.; Han, Q.; Yang, X.; Zhao, F. Study on Force and Wave Energy Conversion Efficiency of Buoys in Low Wave Energy Density Seas. *Energy Convers. Manag.* **2019**, *182*, 191–200. [CrossRef]
28. Hou, H.-M.; Dong, G.-H.; Xu, T.-J.; Zhao, Y.-P. System Reliability Evaluation of Mooring System for Fish Cage Under Ultimate Limit State. *Ocean Eng.* **2019**, *172*, 422–433. [CrossRef]
29. Barrera, C.; Losada, I.J.; Guanche, R.; Johanning, L. The Influence of Wave Parameter Definition Over Floating Wind Platform Mooring Systems Under Severe Sea States. *Ocean Eng.* **2019**, *172*, 105–126. [CrossRef]
30. Pham, H.-D.; Schoefs, F.; Cartraud, P.; Soulard, T.; Pham, H.-H.; Berhault, C. Methodology for Modeling and Service Life Monitoring of Mooring Lines of Floating Wind Turbines. *Ocean Eng.* **2019**, *193*, 106603. [CrossRef]
31. Shen, K.; Guo, Z.; Wang, L. Prediction of the Whole Mooring Chain Reaction to Cyclic Motion of a Fairlead. *Bull. Int. Assoc. Eng. Geol.* **2019**, *78*, 2197–2213. [CrossRef]
32. Ghafari, H.; Dardel, M. Parametric Study of Catenary Mooring System on the Dynamic Response of the Semi-Submersible Platform. *Ocean Eng.* **2018**, *153*, 319–332. [CrossRef]

33. Xue, X.; Chen, N.-Z.; Wu, Y.; Xiong, Y.; Guo, Y. Mooring System Fatigue Analysis for a Semi-Submersible. *Ocean Eng.* **2018**, *156*, 550–563. [CrossRef]
34. Sun, Y.; Sun, Z.; Cao, W.; Xi, G. Numerical Study on Hydrodynamic Characteristics of Moored Offshore Floating Platform. *J. Eng. Thermophys.* **2018**, *39*, 307–313.
35. Whang, J.; Jiao, E.; Zhang, B. Research on Anchoring Model Test of Offshore Steel Aquaculture Platform. *Fish Modern.* **2018**, *45*, 28–33.
36. Johanning, L.; Smith, G.H.; Wolfram, J. Mooring Design Approach for Wave Energy Converters. *Proc. Inst. Mech. Eng. Part M J. Eng. Marit. Environ.* **2006**, *220*, 159–174. [CrossRef]
37. Wei, S.; Wang, Y.; Gao, M. Design of Mooring System for Ultra-Shallow Water Multi-Body Wave Energy Power Generation Device. *Ship Eng.* **2017**, *39*, 70–76.
38. Jiao, E.; Zhang, Y.; Wang, J. Experimental Study on the Mooring of the Pond of the Cage Culture Platform in the South China Sea. In Proceedings of the 2016 Annual Meeting of the Chinese Fisheries Society, Chengdu, China, 3-4 November 2016.
39. Wang, Y.-H.; Wamg, L.; Wang, X.-F.; Xu, S.-W. Numerical Simulation Study on the Mooring System of the Extremely Shallow Semi-Submersible Platform in the South China Sea Islands. *Ship Sci. Tech.* **2017**, *39*, 68–73.
40. Wang, S.; Liu, H.; Guo, G.; Tao, Q.; Huang, X.; Hu, Y. Design of Multi-Point Mooring System for Marine Aquaculture Platform Based on Dynamic Analysis Method. *Trans. Chin. Soc. Agric. Eng.* **2017**, *33*, 217–223.
41. Wu, Z.; Ye, Z.; Cheng, X.; Gao, Y.; Li, C. Analysis of static and dynamic characteristics of tension leg platform for floating offshore wind turbine. *J. Power Eng.* **2016**, *2*, 151–156, 161.
42. Shuo, H.; Yage, Y.; Sheng, S. Numerical Study on the Elastic Mooring System of Shallow-Water Floating Wave Energy Power Generation Devices. In Proceedings of the 27th National Hydrodynamics Symposium, Nanjing, China, 6-11 November 2015.
43. Xiao, Z. Research on the Basic Hydrodynamic Characteristics of Offshore Wind Turbines. Master's Thesis, Hunan University, Changsha, China, 2016.
44. Ni, X.; Cheng, X.; Wu, B.; Wang, X. Coupled Analysis Between Mooring System and VLFS with an Effect of Elastic Deflection of Floater. *Ocean Eng.* **2018**, *165*, 319–327. [CrossRef]
45. CellMed AG. GLP-1 CellBeads®for the Treatment of Stroke Patients With Space-Occupying Intracerebral Hemorrhage. NCT01298830. Available online: http://www.clinicaltrials.gov (accessed on 13 May 2016).
46. Han, L.; Wang, J.; Gao, J. Analysis of Wave Energy Resources in the Sea Areas North of Chu Island, Shandong. *J. Sol. Energ.* **2020**, *41*, 165–171.
47. Fan, T.; Ren, N.; Cheng, Y.; Chen, C.; Ou, J. Applicability Analysis of Truncated Mooring System Based on Static and Damping Equivalence. *Ocean Eng.* **2018**, *147*, 458–475. [CrossRef]
48. Xu, S.; Ji, C.-Y. Dynamics of Large-Truncated Mooring Systems Coupled with a Catenary Moored Semi-Submersible. *China Ocean Eng.* **2014**, *28*, 149–162. [CrossRef]
49. Zhu, G.; Wu, J. Calculation of Mooring Catenary Length Based on Parabola Method. *China W. Transp. (Second Half)* **2013**, *13*, 140–169.
50. Yu, J. Determination of the Length of the Ship's Chain at Anchor. *Tianjin Navig.* **1996**, *2*, 6–8.